BIOCHEMISTRY
including biophysical chemistry & molecular biology

Article

pubs.acs.org/biochemistry

Engineered Streptavidin Monomer and Dimer with Improved Stability and Function

Kok Hong Lim,[†] Heng Huang,[‡] Arnd Pralle,[‡] and Sheldon Park*,[†]

[†]Department of Chemical and Biological Engineering and [‡]Department of Physics, University at Buffalo, State University of New York, Buffalo, New York 14260, United States

Supporting Information

ABSTRACT: Although streptavidin's high affinity for biotin has made it a widely used and studied binding protein and labeling tool, its tetrameric structure may interfere with some assays. A streptavidin mutant with a simpler quaternary structure would demonstrate a molecular-level understanding of its structural organization and lead to the development of a novel molecular reagent. However, modulating the tetrameric structure without disrupting biotin binding has been extremely difficult. In this study, we describe the design of a stable monomer that binds biotin both in vitro and in vivo. To this end, we constructed and characterized monomers containing rationally designed mutations. The mutations improved the stability of the monomer (increase in T_m from 31 to 47 °C) as well as its affinity (increase in K_d from 123 to 38 nM). We also used the stability-improved monomer to construct a dimer consisting of two streptavidin subunits that interact across the dimer−dimer interface, which we call the A/D dimer. The biotin binding pocket is conserved between the tetramer and the A/D dimer, and therefore, the dimer is expected to have a significantly higher affinity than the monomer. The affinity of the dimer (K_d = 17 nM) is higher than that of the monomer but is still many orders of magnitude lower than that of the wild-type tetramer, which suggests there are other factors important for high-affinity biotin binding. We show that the engineered streptavidin monomer and dimer can selectively bind biotinylated targets in vivo by labeling the cells displaying biotinylated receptors. Therefore, the designed mutants may be useful in novel applications as well as in future studies in elucidating the role of oligomerization in streptavidin function.

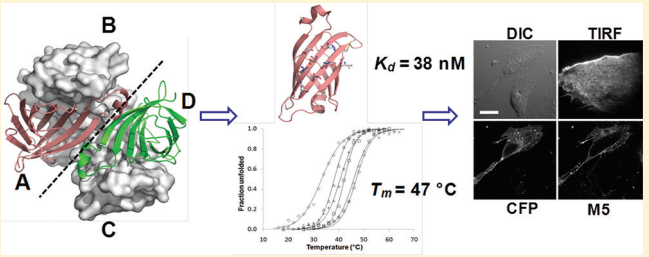

Streptavidin and its avian homologue, avidin, bind biotin with high affinity ($K_d \sim 10^{-15}$ to 10^{-14} M) and are used in molecular detection systems that require stable noncovalent interaction.[1−4] Although they share limited sequence similarity, both molecules adopt a highly conserved tetrameric structure consisting of four identical subunits arranged as two structural dimers. Each of the four subunits in turn forms a common β-barrel motif containing eight antiparallel β-strands. The subunit structure is conserved in all known biotin binding proteins, including the recently identified streptavidin-like molecules from *Bradyrhizobium japonicum* and *Rhizobium etli* (proteobacterium), *Pleurotus cornucopiae* (mushroom), and *Xenopus tropicalis* (frog), which have sequence similarity with streptavidin and avidin in the range of 15−59%.[5−8] The tetrameric architecture is the most common among the streptavidin homologues, suggesting that the tetramer configuration offers advantages over other possible alternatives.[9] In this regard, biochemical studies have demonstrated that tetramerization plays a structurally and functionally important role in this class of molecules.[10−14] However, rhizavidin binds biotin with high affinity as a dimer,[15] suggesting that tetramerization may not be required for high-affinity biotin binding. The binding pockets of rhizavidin include a disulfide bond between the binding loop 3,4 (L3,4) and strand 6,[15] which may contribute to biotin binding by preorganizing the binding pocket.

Designing a functional monomer tests our understanding of the role of oligomerization in streptavidin stability and function and helps extend the reach of streptavidin technology to other novel applications.[16,17] For example, monomeric streptavidin can be used for biotin detection in situations where streptavidin-mediated target aggregation is a concern. In particular, the receptor dimerization is a commonly used mechanism in cell surface signaling,[18] and therefore, labeling cell surface receptors without perturbing cell signaling requires a monovalent reagent. To this end, a monovalent tetramer has been engineered for biophysical studies of the cell receptor dynamics.[19] However, the existing monovalent streptavidin mutants either have limited stability and affinity (monomer) or are cumbersome and wasteful to prepare in vitro (heterotetramer). This has motivated us to propose a structure-based solution and engineer new monomers with improved structural and binding properties to add to the existing repertoire of streptavidin mutants. We show that a combination of a disulfide

Received: July 5, 2011
Revised: August 25, 2011
Published: September 6, 2011

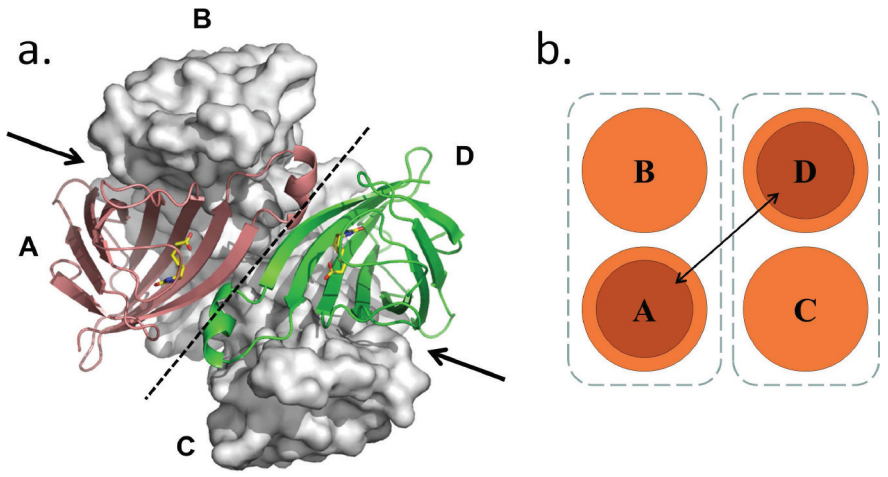

Figure 1. (a) Streptavidin tetramer, which is a D2 dimer of two structural native dimers (A/B and C/D). The dimer interfaces are denoted with arrows, while the tetramer interface, i.e., dimer−dimer interface, is shown as a dotted line. Subunits A and D (ribbons) constitute a functional dimer. Two biotin molecules in the A and D binding pockets are shown as sticks. (b) The double-headed arrow denotes the interactions across the dimer−dimer interface that contribute to tetramerization and biotin binding. The biotin binding pockets located at the top of the A and D subunit β-barrels are highlighted as darker circles. The binding sites of subunits B and C are not shown.

and other rationally designed interfacial mutations can increase the stability of the monomer by up to 16 °C and the affinity by 3-fold compared to those of a monomer that does not contain these designed mutations.

The streptavidin subunits that participate in mutual W120 exchange constitute a functional dimer (subunits A and D in Figure 1), in contrast to the structural native A/B dimer that lacks an obvious link to function (Figure 1). While mutational studies have shown that the interactions across the dimer−dimer interface are important for high-affinity biotin binding,[10,11] interpreting the experimental results is not straightforward because of the multiple roles played by W120. For example, the residue provides direct biotin contacts but also helps stabilize the tetramer conformation.[12,14] We postulated that comparing the biotin affinity of the monomer and A/D dimer should help model the functional role of W120 by decoupling the interactions at the dimer interface from the interactions at the tetramer interface. Because the A/D dimer interface is significantly smaller (buried surface area of 524 Å^2) than the structural dimer interface (1514 Å^2), the formation of the A/D dimer is not observed in solution for wild-type (wt) streptavidin. To construct a stable A/D dimer for biochemical characterization, we cross-linked two monomers using an interchain disulfide bond. Modeling shows that the binding pocket is conserved in the wt tetramer and A/D dimer, and thus, the A/D dimer would also have high biotin affinity. We show that the dimerization results in a significant improvement in the stability and affinity of the molecule. Together, the engineered monomer and A/D dimer may be used to label biotinylated cell surface receptors while minimizing receptor aggregation caused by the tetramer.

MATERIALS AND METHODS

Plasmid Construction. To construct the bacterial expression vector, we amplified the gene corresponding to amino acids 1−139 of mature streptavidin[20] by polymerase chain reaction (PCR) using the primers listed in Table S1 of the Supporting Information and Vent DNA polymerase (all enzymes were purchased from New England Biolabs, unless noted otherwise). The PCR product was digested using NheI and BamHI and ligated with a T7 expression vector derived from pRSET-A digested with the same restriction enzymes.[21] The ligation introduces the streptavidin gene downstream of a six-His tag for affinity purification. All streptavidin constructs also contain a FLAG tag (DYKDDDDK) at the C-terminus for antibody detection of the purified protein. The ligated plasmid was amplified using DH5α cells (Invitrogen, 18265) and sequenced (Roswell Park Cancer Institute, Buffalo, NY).

Protein Expression and Purification. All mutant streptavidin was expressed and purified from bacteria using a protocol modified from that of Howarth et al.[19] We transformed *Escherichia coli* T7 Express *lysY* competent cells (New England Biolabs, C3010) with the mutant plasmids and selected the transformants on LB plates containing 100 μg/mL ampicillin (IBI Scientific, IB 02040). Overnight, a 5 mL LB culture was inoculated from four to six colonies and diluted 100-fold into 250 mL of LB medium the next day. The cultures were grown to an OD_{600} of 0.8−1.0 and induced with 100 μM isopropyl β-D-thiogalactopyranoside (Boston BioProduct, P806) for 4 h at 37 °C. To isolate streptavidin from the inclusion body, the cells were harvested and resuspended in 5 mL of B-PER (Thermo Scientific, 78248), vortexed for 1 min, and centrifuged at 12000 rpm for 20 min. The pellet was suspended in 5 mL of B-PER with 400 μg/mL lysozyme (Affymetrix-USB, 18645) and incubated at 20 °C for 5 min. A 20 mL amount of wash buffer WB1 containing 50 mM Tris-HCl (Fisher Scientific, BP 154) (pH 8.0), 100 mM NaCl (Fisher Scientific, S271), and 0.5% Triton X-100 (Sigma, T8787) was added to the suspension and the mixture vortexed until the solution became homogeneous, and the mixture was spun at 12000 rpm to sediment the inclusion body. The pellet was washed twice more in WB1 and dissolved in 1.5 mL of solubilization buffer [6 M guanidine hydrochloride (Mallinckrodt Baker, 3818), 50 mM Tris-HCl (pH 8.0), and 100 mM NaCl]. The insoluble fraction was removed by centrifugation, and the supernatant was mixed with 250 μL of TALON metal affinity resin (Clontech, 635502) for six-His affinity purification. After incubation at 20 °C for 1 h with occasional stirring, the resin was washed twice in 1.5 mL of resin wash buffer (WB2) [6 M guanidine hydrochloride, 50 mM Tris-HCl (pH

dx.doi.org/10.1021/bi2010366 | *Biochemistry* 2011, 50, 8682−8691

7.0), 150 mM NaCl, and 50 mM imidazole (Sigma-Aldrich, I2399)] and eluted in 3 × 500 μL of elution buffer (EB) [6 M guanidine hydrochloride, 50 mM Tris-HCl (pH 7.0), 150 mM NaCl, and 300 mM imidazole]. The elution fractions were added drop by drop to 40 mL of ice-cold refolding buffer (RB) [50 mM Tris-HCl (pH 8.0), 150 mM NaCl, 0.3 mg/mL D-biotin (Anaspec, 21101), 0.2 mg/mL oxidized glutathione (Acros Organics, AC 32022), and 1 mg/mL reduced glutathione (Affymetrix-USB, 16315)] under rapid stirring to refold the protein. The precipitates were removed by centrifugation. The refolded protein was concentrated to 2 mL using Amicon Ultra centrifugal filters (Millipore, UFC 801024) with a 10 kDa cutoff. The concentrated protein was transferred to FloatALyzer G2 dialysis device (Spectrum Laboratories, G235031) with an 8−10 kDa cutoff and dialyzed three times against 2 L of dialysis buffer (DB) [50 mM Tris-HCl (pH 8.0) and 150 mM NaCl] at 4 °C over 2 days.

Gel Filtration. Dialyzed protein samples were spun at 14000 rpm to remove precipitates, and the supernatant was analyzed on a Superdex 75 10/300 GL column pre-equilibrated in 50 mM sodium phosphate (pH 7.0) and 150 mM NaCl (GE Healthcare, 17-5174) using the ÄKTAprime plus workstation (GE Healthcare). The elution profile was analyzed using the manufacturer's PrimeView 5.0 evaluation software. To calculate the molecular mass, a reference set of protein markers (Sigma, MWGF70) was run for calibration. The elution fractions were combined and analyzed on 14% SDS−PAGE gel to check the purity.

Circular Dichroism Spectroscopy. The circular dichroism spectra were recorded on a J-715 CD spectropolarimeter (JASCO) with a temperature controller using a cuvette with a path length of 1 mm. A spectral bandwidth of 1 nm was used for data collection. Streptavidin mutants were prepared in PBS (pH 7.4) at a concentration of 5 μM. To induce heat denaturation, the temperature was increased from 4 to 96 °C, and the CD spectra were recorded between 200 and 250 nm for every 2 °C increment. The fraction of denatured protein was fitted to the integrated form of the van't Hoff equation[21] to obtain the transition enthalpy (ΔH_{vH}) and the melting temperature (T_m).

Affinity Measurement. The dissociation constant (K_d) was measured by fluorescence polarization using fluorescein biotin (FB) (AnaSpec, 60656). The concentration of the purified proteins was determined on the basis of UV absorption. A titrating amount of the protein was mixed with 100 nM FB in 1 mL of PBS (pH 7.4) with 0.01% bovine serum albumin (Sigma, A7906) (PBSA). After overnight incubation at 4 °C, the polarization was measured using a cuvette with a path length of 10 mm on a QuantaMaster fluorescence spectrofluorometer (Photon Technology International). The fraction of bound FB was determined on the basis of the degree of fluorescence polarization and fitted to the quadratic binding equation using Matlab, as described in ref 21.

Flow Cytometric Analysis of Biotin Binding. To test for biotin binding by flow cytometry, we mixed 10 μM purified proteins with 1 μL of biotin-coated microspheres (Bangs Laboratories, CP10N) in 50 μL of PBSF [PBS (pH 7.4) with 0.1% BSA]. The mixture was incubated for 1 h at 37, 42, or 55 °C, and the beads were washed in 500 μL of PBSF twice to remove unbound protein. To quantify the proteins on the beads, the beads in 40 μL of PBSF were labeled with 1 μL of monoclonal mouse anti-FLAG antibody (Stratagene, 200472) for 1 h at 20 °C, followed by labeling for 30 min on ice with 2 μL of fluorescein isothiocyanate (FITC)-conjugated goat anti-mouse IgG antibody (Sigma, F0257).

To determine if the A/D dimer can bind two ligands simultaneously, we performed coprecipitation using purified A/D and biotinylated ligand. We incubated A/D with biotinylated rabbit anti-TNF antibody (b-αTNF) (BD Biosciences, 557432) or biotinylated phycoerythrin (b-PE) (Invitrogen, P-811) for 1 h at 20 °C and used 1 μL biotin-coated microspheres to pull down the complex over 1 h on ice. The beads were then washed twice in 500 μL of PBSF and labeled with anti-FLAG antibody and FITC-conjugated goat anti-mouse IgG antibody to quantify bound A/D or FITC-conjugated goat anti-rabbit IgG antibody to quantify bound b-αTNF (Sigma, F0382). The labeled microspheres were analyzed with BD FACSCalibur (Becton Dickinson). The histogram overlays were generated using CXP Analysis software version 2.2 (Beckman Coulter).

Dynamic Light Scattering. The hydrodynamic radii of the mutants were obtained on a Zetasizer Nano ZS90 dynamic light scattering analyzer (Malvern). BSA and egg white lysozyme were run for comparison. The purified proteins (1 mg/mL in PBS) were passed through a 0.2 μm filter (Corning, 431229) immediately prior to measurement. The size distribution profile was computed on the basis of the scattered light intensity using the manufacturer's Zetasizer version 6.0.

Molecular Dynamics Simulation. Simulation was performed with NAMD version 2.6[22] with the Charmm 27 force field[23] using Protein Data Bank entry 1SWE as the starting coordinates.[21] Briefly, streptavidin tetramer or monomer (chain A containing QMA mutations) was immersed in a water box with a 12 Å separation to the nearest wall; 100 mM NaCl was used to neutralize the net charge in the system. Water molecules were first energy minimized for 5000 steps with the protein fixed, and then the entire system was relaxed for another 5000 steps. For the simulation, the temperature of the system was increased to the final temperature of 310 K over 1.55 ps. The simulation was conducted under constant pressure (1 atm) and temperature (NPT ensemble) using 1 fs time steps under periodic boundary conditions. Electrostatics were treated using the particle mesh Ewald sum. Both simulations were performed for 10 ns, and the trajectories were visualized and analyzed using VMD.[24]

To compute the residue-specific root-mean-square deviation (rmsd) of main chain atoms, the simulated structures were translated and rotated as a rigid body to superimpose simulated structures of subunit A with its starting structure. The rmsd values corresponding to 1−10 ns were averaged. Similarly, the simulated structures of subunits B−D were moved to superimpose them with their respective starting coordinates to compute their rmsd. The rmsd values of identical residues from the four subunits were averaged to obtain the tetramer rmsd. The monomer rmsd values were similarly computed.

Cell Culture. Potorous tridactylis kidney (PtK2) cells were cultured in Eagle's minimum essential medium (EMEM) supplemented with 10% fetal bovine serum and 1% penicillin/streptomycin (Invitrogen) at 37 °C under 5% CO_2. For imaging, cells were seeded sparsely on 18 mm glass coverslips and cotransfected with an equal amount of plasmids encoding AP-CFP-TM (in pDISPLAY vector) and BirA-ER (pDISPLAY) using Lipofectamine 2000 (Invitrogen) 24 h after plating. The medium was then supplemented with 5 μM D-biotin (Biotium, Inc.) to ensure biotinylation of AP-CFP-TM on cell membrane. Labeling and imaging were conducted 24 h after transfection (both vectors were gifts of A. Ting,

Massachusetts Institute of Technology, Cambridge, MA).[25] For live cell TIRF imaging, the cells were washed three times with Dulbecco's modified Eagle's medium supplemented with 10 mM HEPES (HDMEM) to eliminate free biotin before labeling with the Alexa Fluor 488-conjugated M5 monomer or A/D dimer or wt tetramer (each at 2 μM) at room temperature for 5 min. The coverslip was then washed and mounted in HDMEM for imaging. For confocal imaging, the cells were washed three times with PBS before being fixed with 4% paraformaldehyde (PFA) for 15 min at room temperature. They were then washed with PBS twice before being incubated with M5, A/D, or wt streptavidin (2 μM in all cases) for 5 min at room temperature. After the samples had been briefly washed with PBS, labeling with 1 μL of monoclonal mouse anti-FLAG antibody (for M5 and A/D dimer) or 1 μL of monoclonal mouse anti-streptavidin (Abcam, ab10020) (for wt tetramer) was performed on ice (4 °C) for 1 h, followed by incubation with 2 μL of fluorescein isothiocyanate (FITC)-conjugated goat anti-mouse IgG antibody on ice (4 °C) for 30 min. The coverslips were then washed with PBS and mounted on glass slides in glycerol for confocal imaging.

Imaging. To prepare mutant and wt streptavidin for cell labeling, we labeled them with a fluorescent dye. We mixed 20 μM protein in PBS with 5 μM Alexa Fluor 488 5-SDP ester (Invitrogen, 30052) in a reaction volume of 100 μL for 2 h at 20 °C. The molar ratio between the dye and the protein was kept low to prevent conjugation of multiple dye molecules, which may destabilize the protein. Upon completion of conjugation, the unreacted dye was removed by dialyzing twice against 2 L of PBS buffer using Slide-A-Lyzer MINI Dialysis Units with a 10 kDa cutoff (ThermoScientific, 69570). The efficiency of dye conjugation was analyzed based on the difference of mobility between conjugated and unconjugated protein determined on a 12% SDS–PAGE (data not shown).

TIRF imaging was performed using an objective-type TIRF microscope constructed around an inverted microscope (AxioObserver, Zeiss) and an EMCCD camera (Andor iXon+ 897). The 488 nm line from an argon–krypton laser (Coherent) was sent through the objective (Zeiss, oil immersion, NA = 1.45) at TIRF angle to excite Alexa Fluor 488 fluorescence from the bottom cell membrane. TIRF images were taken with the EMCCD and accumulated over 1 s. Fixed cells were imaged using a confocal microscope (Zeiss, LSM710) with sequential acquisitions of CFP fluorescence (from AP-CFP-TM, 405 nm excitation), FITC fluorescence (from Alexa Fluor 488-conjugated secondary antibody, 488 nm excitation), and DIC images. All imaging was performed at room temperature.

RESULTS

Stability-Enhanced Monomers. Monomeric streptavidin containing four sterically hindered interfacial mutations, QM (T76R, V55T, L109T, and V125R), has been previously reported.[26] Because monomeric streptavidin exposes W120 to the solvent, we also mutated the residue to Ala and used the resulting monomer, QMA, as the starting point of our investigation to engineer a stable and functional monomer. For the purpose of this study, QMA is termed the wt monomer.

Streptavidin contains a flexible binding loop L3,4 (residues 45–52) near the binding pocket that undergoes an open-to-closed conformational transition on biotin binding.[27,28] A 10 ns molecular dynamics simulation shows that the residue-specific rmsd values for the loop residues are larger in the monomer than in the tetramer, where the loop residues are in part stabilized through the interaction with W120 (Figure 2).

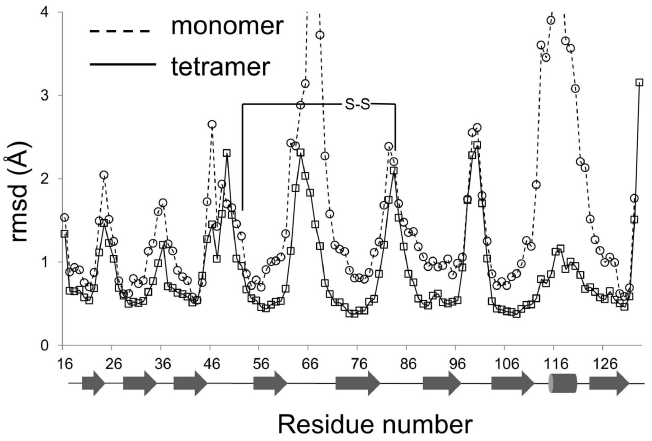

Figure 2. Residue-specific rmsd of QMA (---) and tetramer (—) calculated on the basis of 10 ns molecular dynamics simulations. The secondary structural assignment is indicated below the *x*-axis. A disulfide was engineered between S52C and Y83C (–S–S–) to reduce the flexibility of the binding loop.

Restricting the movement of the loop may increase the stability of the molecule and also increase its biotin affinity by reducing the conformational flexibility within the binding pocket. To test if a disulfide in the binding pocket would increase the stability and/or affinity of streptavidin, we selected two potential pairs of cysteine mutations based on simulated structures: (i) E51C and Y83C (M1) or (ii) S52C and Y83C (M2) (Table 1). We expressed and purified the two mutants and QMA from bacterial inclusion bodies. The purified proteins run as single bands on an SDS–PAGE gel with or without DTT, showing that the cysteine residues of M1 and M2 do not form nonspecifically cross-linked aggregates (data not shown). We characterized the stability of the mutants by circular dichroism spectroscopy. Both disulfide-containing mutants were more stable than QMA by 5.8–6.6 °C (Table 2), but M2 exhibited a sharper transition from folded to unfolded states and was thus selected for further study.

Using M2 as a template, we introduced additional mutations at the dimer interface to improve its stability further. Because the native dimer interface contains a large number of polar residues, we concluded that hydrophobicity is not a serious impediment to monomer stability. We therefore tested if the stability can be improved by introducing salt bridges and replacing low β-sheet propensity residues with higher β-sheet propensity residues. In this regard, we mutated G74 to E to increase the β-sheet propensity at the position.[29] In the wt dimer, G74 of one subunit functions as a "hole" residue to the "knob" residue T76 of the other subunit.[21] Thus, the G74E mutation, combined with the T76R mutation of QMA, would further ensure monomer formation by creating steric repulsion as well as by potentially forming an intramolecular salt bridge. The mutation increased the stability of the monomer to 43.6 °C (T_m).

Encouraged by these results, we engineered additional salt bridges by introducing four more mutations at the dimer interface, A72K, A89R, T91E, and S93R. The charged residues were distributed to maximize the number of salt bridges formed between neighboring charged residues. The substitutions also replace small residues with larger residues, which are more

dx.doi.org/10.1021/bi2010366 | *Biochemistry* 2011, 50, 8682–8691

Table 1. Mutants Discussed in This Study[a]

	E51	S52	V55	A72	G74	T76	K80	Y83	N85	H87	A89	T91	S93	L109	T111	G113	W120	V125
QMA			T			R								T			A	R
M1	C		T			R		C						T			A	R
M2		C	T			R		C						T			A	R
M2.1		C	T			R		C		C				T		C	A	R
M2.2		C	T			R	C	C	C					T			A	R
M3		C	T		E	R		C						T			A	R
M4		C	T			R		C			R			T	E		A	R
M3.1		C	T		E	R		C			R			T	E		A	R
M5		C	T	K	E	R		C			R	E	R	T			A	R
M6		C	T	K	E	R		C			R	E	R				A	R
M7		C		K	E	R		C			R	E	R				A	R
A/D		C		K	E	R		C			R	E	R					C

[a]The wt residues are shown at the top, and the specific mutations are shown underneath for each mutant.

Table 2. Measured T_m and K_d Values of Mutant and wt Streptavidin[a]

	T_m (°C)	K_d (nM)
QMA	31.0 ± 1.0	123.0 ± 6.6
M1	36.8 ± 0.3	110.5 ± 8.1
M2	37.6 ± 1.3	64.4 ± 4.7
M2.1	not folded	–
M2.2	37.7 ± 1.0	145.2 ± 16.4
M4	37.7 ± 0.6	88.4 ± 6.7
M3.1	42.9 ± 0.5	69.5 ± 6.0
M3	43.6 ± 0.6	44.6 ± 3.5
M5	46.7 ± 0.2	38.2 ± 2.2
M6	41.4 ± 0.9	52.2 ± 4.2
M7	40.2 ± 0.2	43.6 ± 3.7
A/D	47.0 ± 0.1	17.4 ± 0.3

[a]The measurements were conducted in triplicates, and the standard errors of the mean are given.

effective in stabilizing the underlying β-barrel conformation.[30] The purified protein runs as a monomer on SDS–PAGE (Figure 3a) and elutes as a single peak from a gel filtration

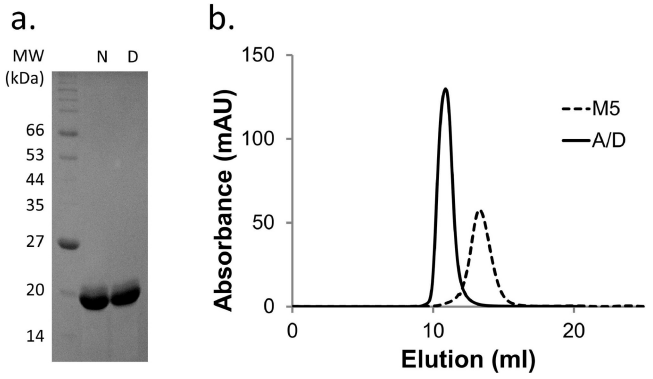

Figure 3. (a) Purified M5 was analyzed by SDS–PAGE. N, loaded without boiling; D, boiled in 5 mM DTT before being loaded. This comparison is useful because wt streptavidin runs as a tetramer if loaded without boiling and as a monomer if loaded after boiling.[10,21] (b) Elution profiles of M5 (---) and the A/D dimer (—) from a Superdex 75 gel filtration column show that they adopt a homogeneous conformation in solution.

column, although the computed molecular mass of 26.5 kDa is higher than the theoretical value of 17 kDa (Figure 3b). The discrepancy may be due to disordered residues at both termini, which increase the effective radius of gyration. CD spectroscopy confirmed that the engineered M5 has a T_m of 46.7 °C (Figure 4, Figure S1 of the Supporting Information, and Table

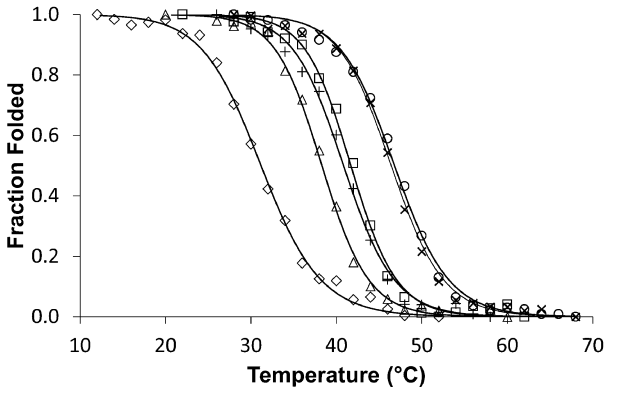

Figure 4. Thermal stability of the mutants determined by circular dichroism spectroscopy. QMA has an anomalous transition between 210 and 220 nm, which prevents it from being fitted using a two-state transition model. Instead, we fitted the measurements at 231 nm to a two-state transition, taking advantage of the fact that the thermal transitions of wt streptavidin measured at 205, 216, and 231 nm all agree with the known melting temperature, 75 °C[21,51,52] (also see Figure S1 of the Supporting Information). Therefore, fitting the values at 231 nm provides a useful surrogate for stability measurement of streptavidin variants, when the analysis at a more conventional wavelength is not possible. Legend: (◇) QMA, (△) M2, (+) M7, (□) M3, (×) M5, and (○) A/D dimer.

2), which to the best of our knowledge is the highest stability that has been achieved for a monomer. We reverted some of the mutations to wt residues to test if we may have inadvertently introduced destabilizing mutations, but none of the mutants we tested had a melting temperature higher than that of M5, suggesting that the mutant does not appear to contain a mutation that is overtly destabilizing.

Affinity Measurements. The biotin affinity of the mutants was then measured with a fluorescence polarization assay using biotinylated fluorescein as the ligand (Figure 5). The molecule contains a 14-atom spacer between the fluorophore and biotin to ensure that we are measuring the affinity of the biotin–streptavidin interaction. The wt monomer has a K_d of 123 nM as demonstrated by this assay (the affinity of QM was previously reported to be 186 nM[26]). We tested if

dx.doi.org/10.1021/bi2010366 | Biochemistry 2011, 50, 8682–8691

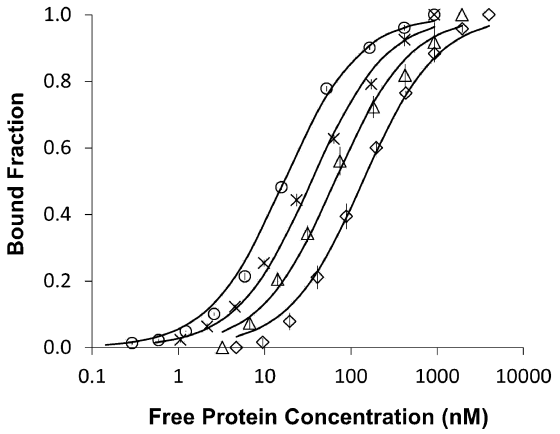

Figure 5. Binding affinity of the mutants determined by fluorescence polarization spectroscopy using biotinylated fluorescein as a probe. The quadratic binding curve was fit to normalized polarization as a function of free protein concentration: (◇) QMA, (△) M2, (×) M5, and (○) A/D dimer.

the stability-enhanced mutants bind biotin with higher affinity by reducing the entropic penalty associated with binding.[31,32] For example, the catalytic sites of enzymes often exhibit high structural stability because it allows preorganization of the binding site to optimize substrate binding.[33] Consistent with the expectation, the highest affinity was observed for the mutant with the highest stability, M5, which bound with a K_d of 38.2 nM (Table 2). For the mutants with a smaller increase in T_m, the change in affinity was correspondingly small. However, the correlation between stability and affinity was weak, because the improvement in affinity was modest (2−3-fold) and some mutations increased the stability but lowered the affinity.

Characterization of the A/D Dimer. A functional streptavidin dimer is expected to bind streptavidin with high affinity, because its binding pocket preserves essential biotin contacts (see Figure 1). However, this hypothesis cannot be tested directly using wt streptavidin, because the molecule spontaneously forms a tetramer. Instead, we used the designed monomer M7 to construct a stable functional dimer. Because the dimer interface buries a relatively small surface area (524 Å^2), we mutated V125 to C to cross-link the dimer with a disulfide. Intermolecular disulfide cross-linking requires specific intermolecular interaction and is used in drug screening, structural biology, and protein interaction studies.[34−37] The two V125 residues of the modeled A/D dimer are separated by a C_β−C_β distance of 4.2 Å, which can be easily bridged with a disulfide (Figure 6a).

We refolded M7 containing C125 in a buffer containing different concentrations of reduced and oxidized glutathione to obtain a nearly complete cross-linking of the monomer (Figure 6b). The dimer eluted from the gel filtration column as a single peak with a predicted molecular mass of 49.1 kDa (Figure 3b). This is higher than the theoretical molecular mass of 34 kDa, but the discrepancy may have been caused by disordered terminal residues as well as the large radius of gyration because of the structural asymmetry in the molecule (21.2 Å compared to 17.0 Å for a structural dimer). Dynamic light scattering (DLS) shows that the dimer forms a monodisperse sample in solution (Figure S2 of the Supporting Information), suggesting that the molecule does not form large aggregates. The stability of the dimer (T_m = 47.0 °C) was higher than that of M7 by ∼7 °C. The increase in stability may be due to the burial of hydrophobic residues at the interface, including L25, V47, and L124, as well as the presence of a disulfide bond. An affinity measurement by FP shows that the dimer has a K_d of 17.4 nM at 4 °C, which is 7-fold higher than that of QMA, although still significantly lower than that of the wt tetramer (Figure 5 and Table 2). The affinity of the dimer remained unchanged at 20 °C (K_d = 18.5 ± 1.2 nM), consistent with the high thermal stability of the molecule. Finally, addition of 10 mM DTT reduced both the stability of the dimer (T_m = 32.6 ± 0.4 °C) and its biotin affinity at 4 °C (K_d = 142.0 ± 1.6 nM), showing that the disulfides are important for stability and function.

Bead Binding Assay. To demonstrate temperature-dependent biotin binding of the designed monomer and dimer, we incubated M7 and A/D dimer with biotinylated microbeads at temperatures ranging from 25 to 55 °C. After the unbound protein was washed away, the beads were analyzed by flow cytometry to quantify the amount of bound streptavidin.

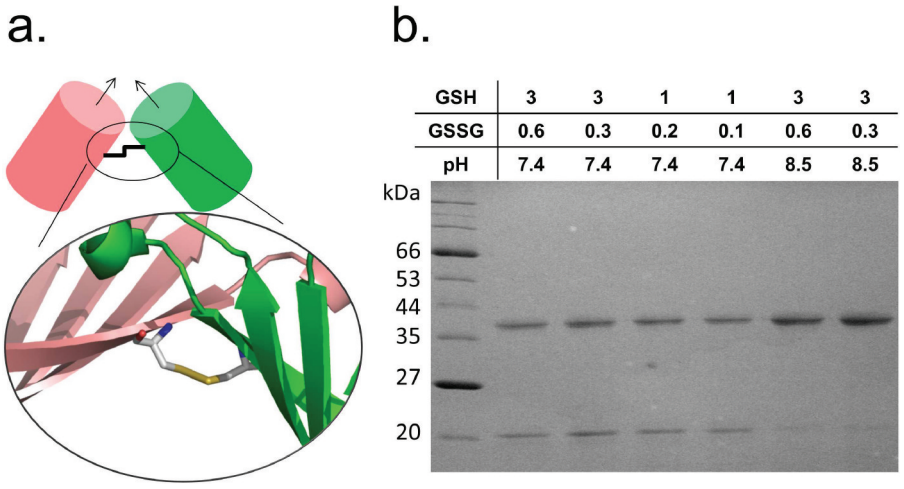

Figure 6. (a) Schematics of the A/D dimer. The view is rotated by 90° with respect to Figure 1 to show a side view of the dimer. The inset shows the modeled disulfide bond. The arrows correspond to the binding pocket at the end of the β-barrel. (b) A/D dimer formation was optimized by varying the ratio of reduced (GSH) to oxidized glutathione (GSSG) and the buffer pH to obtain nearly complete cross-linking. The concentration of glutathione is shown in millimolar.

dx.doi.org/10.1021/bi2010366 | Biochemistry 2011, 50, 8682−8691

Both proteins bound the beads well at temperatures below their measured T_m (Figure 7a,b). However, the amount of bound protein systematically decreased as the temperature was increased, until little protein remained bound at temperatures significantly above their respective melting temperatures. Preblocking the A/D dimer with free biotin quenches its ability to bind the beads in a concentration-dependent manner, showing that the interaction is specific (Figure 7c).

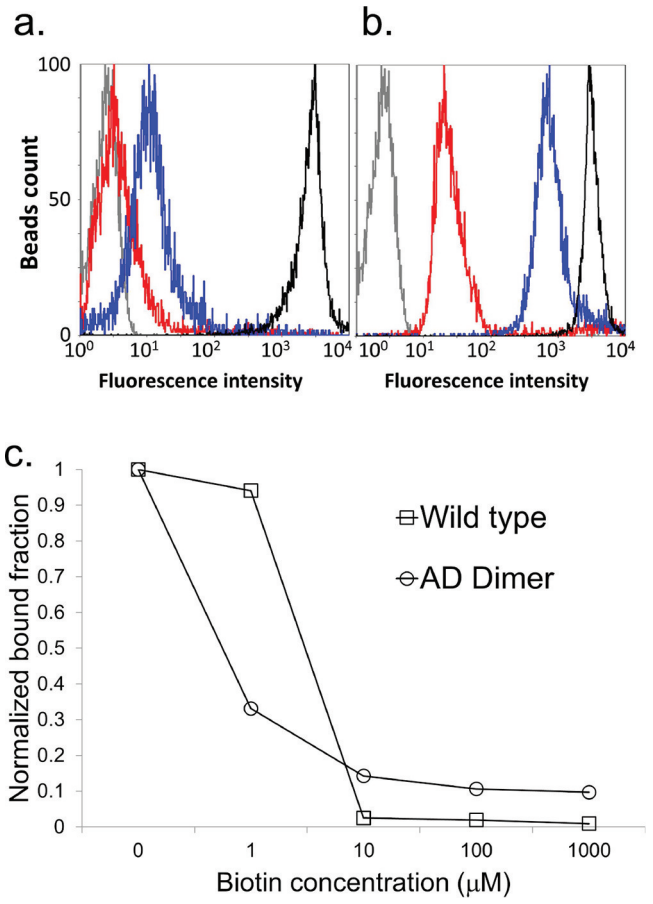

Figure 7. Purified M7 (a) and the A/D dimer (b) were tested for biotin binding by mixing them with biotinylated microbeads at 37 (black), 42 (blue), and 55 °C (red). The intensity at 25 °C (not shown) is essentially the same as that at 37 °C. After washing the beads to remove unbound protein, the beads were then equilibrated at 4 °C and labeled with anti-FLAG antibody and FITC-conjugated secondary antibody for analysis by flow cytometry. The gray trace shows data for beads labeled with the primary and secondary antibody alone. (c) To demonstrate specific binding of the wt tetramer and A/D to biotin beads, each protein (monomer concentration of 6 and 24 μM for wt and A/D, respectively) was preincubated with varying concentrations of free biotin at 4 °C for 1 h before addition of biotinylated beads. The amount of streptavidin bound to the beads was then quantified by flow cytometry and normalized using the mean fluorescence intensity (MFI) with respect to the sample without biotin.

Application of Engineered Mutants in Cell Labeling. To demonstrate an in vivo application of the engineered molecules, we tested them in a cell biology experiment to detect biotinylated receptors on the cell surface. We transiently transfected PtK2 cells with two expression vectors for a cell membrane protein[19] and the bacterial biotin ligase BirA. The receptor contains a 15-amino acid biotin acceptor protein (AP) sequence fused at the N-terminus for in vivo biotinylation by BirA. The AP sequence is fused to a cyan fluorescent protein (CFP) and the transmembrane domain (TM) of the platelet-derived growth factor receptor (PDGF-R) for membrane targeting. The cells displaying the biotinylated receptor were then labeled with M5, A/D dimer, or wt tetramer and visualized using anti-FLAG antibody (M5 and A/D) or anti-streptavidin antibody (wt tetramer) and a fluorescently labeled secondary antibody. Confocal fluorescence images show that the cells expressing the receptor are preferentially labeled with both wt and engineered streptavidin (Figure 8).

Wt tetrameric streptavidin is commonly used for detection and labeling, but it aggregates mobile (e.g., soluble or diffusing in the lipid bilayer) ligands by cross-linking them. The receptors that oligomerize during their normal function are especially susceptible to clustering artifacts during labeling studies. Because a monomer does not cross-link the ligands, it could be a useful reagent for biotin detection in these cases. To test if a monomer binds the biotinylated membrane proteins without aggregating them, we labeled live PtK2 cells with the Alexa Fluor 488-conjugated monomer, dimer, and tetramer and analyzed the membrane distribution of labeled protein by total internal reflection fluorescence microscopy (TIRF). While wt tetramer induces the formation of large aggregates, M5 labeled the cells without causing large aggregates. This is consistent with the binding of M5 to the individual receptors without cross-linking. Some aggregation was observed when the cells were labeled with the dimer, although the degree of aggregation was not as pronounced as with the tetramer.

DISCUSSION

The coupling between protein oligomerization and function is common in nature, and contributes to the functional loss that sometimes results from disrupted quaternary structure.[38,39] Similarly, the streptavidin and avidin monomers that have been engineered to date all have an affinity that is significantly lower than that of wt tetramer.[16] An engineered single-chain dimer similarly binds biotin weakly,[40] although its affinity for biotin-4-fluorescein was reported to be high. More importantly, however, the limited stability and solubility of the designed monomer (e.g., T_m = 31 °C for QMA) is a hindrance in many experiments, which has motivated our study to design a monomer with improved stability for exploring new applications based on the biotin−streptavidin interaction.

It is important to optimize protein stability for in vivo applications. For example, M5 and M7 both have similar affinities in vitro, but labeling the cells with M5 (T_m = 47 °C) resulted in significantly less nonspecific binding than with M7 (T_m = 40.2 °C) (data not shown). To improve stability, we replaced short interfacial residues (A72, G74, T76, A89, T91, and S93) with longer charged residues (K72, E74, R76, R89, E91, and R93). These residues were targeted because small amino acids, with the exception of T, are typically poor β-sheet formers,[41−43] whereas large residues and branched amino acids can use their bulky side chains to shield the main chain from the bulk solvent and thus stabilize the main chain hydrogen bonds.[30] Although Gly has the lowest β-sheet propensity, G74 serves an important structural role in the dimer by interacting with T76 of the complementary subunit to form a "knob-into-hole" pair.[21] Because interfacial packing is not relevant in a monomer, the presence of a Gly without the benefit of favorable steric packing appears to have an overall destabilizing effect on the structure. This interpretation is supported by the

dx.doi.org/10.1021/bi2010366 | Biochemistry 2011, 50, 8682–8691

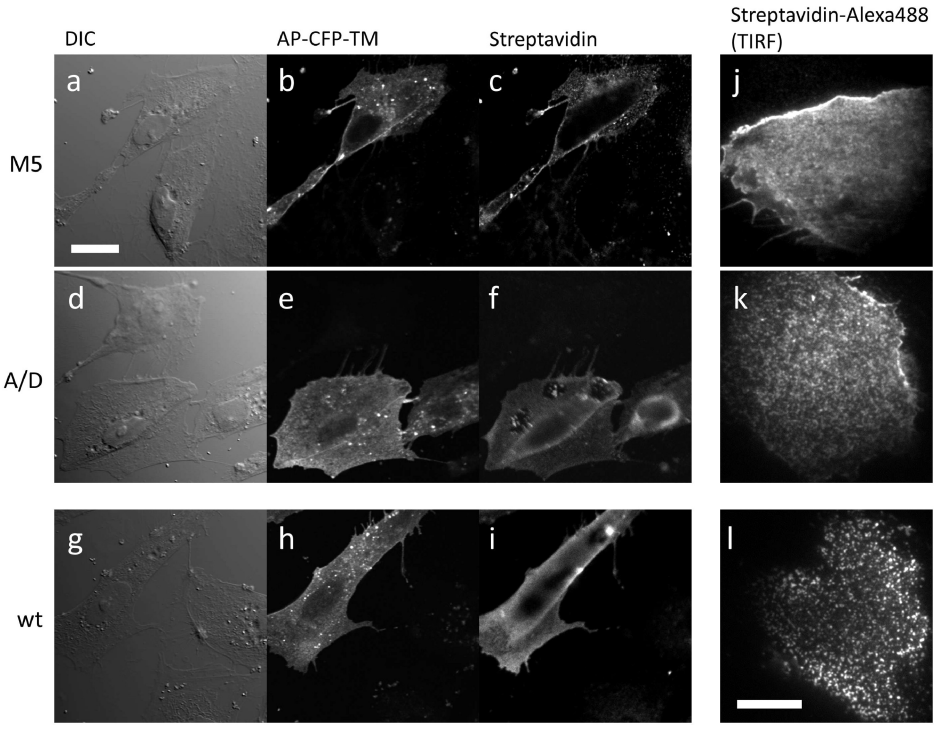

Figure 8. Specific binding of M5, A/D dimer, and wt tetramer to a biotin-presenting PtK2 cell membrane. PtK2 cells expressing the biotinylated cell receptor, AP-CFP-TM, were fixed and labeled using M5 (top), A/D dimer (middle), or wt tetramer (bottom). The bound streptavidin was visualized using anti-FLAG (mutants) or anti-streptavidin (wt) antibody and FITC-conjugated secondary antibody. DIC (a, d, and g), CFP fluorescence (b, e, and h), and FITC fluorescence (c, f, and i) micrographs were taken using a confocal microscope (scale bar of 20 μm). Among the cells within the field of view, as visible in DIC images, only the ones expressing biotinylated AP-CFP-TM have streptavidin specifically bound to the cell membrane. Live cells were labeled with Alexa Fluor 488-conjugated M5, A/D, and wt tetramer and imaged using TIRF microscopy to evaluate streptavidin-induced clustering of biotinylated ligands (j–l, scale bar of 10 μm). The cells labeled with wt tetramer (l) show optically resolvable clusters, which are absent in M5-labeled cells (j).

large increase in monomer stability resulting from the G74E mutation.

Predicting the contribution of individual surface salt bridges is challenging and requires knowledge of thermodynamic quantities that are difficult to estimate accurately.[44,45] Instead, we assumed that surface positions can accommodate many different mutations and applied heuristic modeling to identify the mutations that improve stability. In this regard, we introduced several independent stabilizing mutations, which appear to have cumulative effects on stability.[46,47] The stability of the final design (M5) may be analyzed in terms of incremental contributions from various sources that can be estimated by comparing the T_m values of different mutants. For example, the disulfide between S52C and Y83C contributes a ΔT_m of 6.6 °C based on a comparison of QMA and M2. Replacing G74 with E improves the stability by an additional 6 °C by increasing the secondary structural propensity and by creating a potential salt bridge with T76R. Because the charged residue substitutions A72K, S89R, T91E, and S89R together contribute a ΔT_m of 3.1 °C, which is less than the improvement from the G74E mutation alone, optimizing the secondary structural propensity appears to be more critical than introducing new electrostatic interactions. The substitution of two hydrophobic interfacial residues with polar residues, V55T and L109T, together stabilizes the monomer by 6.5 °C, which is consistent with the observation that polar substitutions on the surface are typically stabilizing.[48] The bulk of this stability improvement is contributed by L109T (based on a comparison of M5−M7), which may also reflect the difference in the β-sheet propensity of L, V, and T. Likewise, a combination of van der Waals contacts and hydrogen bonds at the A/D dimer interface contributes ~7 °C to the stability to the molecule.

Our study shows that the interactions at the dimer interface contribute only weakly to function, because the mutations that improve the stability by up to ~16 °C improve the affinity by only a few-fold. It was surprising that the A/D dimer has an affinity that is still many orders of magnitude lower than that of the wt tetramer. Together, these mutants suggest that the interactions at the native dimer and the A/D dimer interfaces individually do not support high-affinity biotin binding, but together they can increase the affinity by 10^6–10^7-fold. Although the existence of subunit cooperativity has been suggested,[49] no model exists yet to explain extensive structural coupling. Nonetheless, it is tempting to think that in the tetramer the B subunit may help couple the interactions at the A/D interface with other interactions within the binding pocket. For example, if the L4,5 residues 63-APATDGS-69 of the B subunit are stabilized by the A/D interaction, they can in turn help organize the binding pocket by contacting the L5,6 loop of the A subunit. It should be possible to test this hypothesis by deleting the L4,5 residues from the tetramer and demonstrating weakened biotin binding. Irrespective of the details of the model, however, a comparison of the engineered monomer and dimer mutants with the wt tetramer suggests that the interactions at the A/D dimer interface alone are insufficient to achieve high affinity, and the native tetrameric structure is essential for wt activity.

dx.doi.org/10.1021/bi2010366 | *Biochemistry* 2011, 50, 8682–8691

Although wt streptavidin has four identical biotin binding sites, a previous study has suggested that the two adjacent biotin binding sites are anticooperative because the binding of a ligand at one site disfavors the binding at the adjacent binding site through steric repulsion.[50] For example, we noticed that the A/D dimer does not cluster cell surface receptors as much as wt streptavidin, suggesting that only one binding site may be active at a time. If true, A/D dimer may well function as a monovalent dimer, despite having two functioning binding sites. We tested whether the A/D dimer can bind two biotinylated targets simultaneously by mixing the dimer with a biotinylated anti-TNF antibody (b-αTNF) or biotinylated phycoerythrin (b-PE), and using biotinylated beads to pull down the streptavidin–ligand complex. If A/D is able to bind two biotinylated ligands simultaneously, the beads would pull down both streptavidin and b-αTNF/b-PE. Flow cytometry analysis confirms the presence of both b-αTNF and b-PE on the beads, showing that the A/D dimer can simultaneously bind two biotinylated substrates (Figure S3 of the Supporting Information). The amount of A/D also decreases when it is preincubated with b-αTNF (Figure S3a of the Supporting Information, samples 3 and 4) or b-PE (Figure S3b of the Supporting Information, iii and iv), but because these pull-down assays are not designed to be quantitative, they do not distinguish between simple quenching of streptavidin activity and anticooperativity. The reduced level of clustering of membrane proteins labeled with A/D may thus be a consequence of its lower affinity compared to that of wt, which reduces the probability of simultaneously binding two targets under the conditions of excess streptavidin. Importantly, recognition of soluble biotinylated ligands while minimizing aggregation is a feature of A/D that may prove useful during in vivo applications.

SUMMARY

In this study, we have described the construction of stable streptavidin monomer and dimer by rational design. The study was motivated by the current lack of a stable monomer for in vivo applications. Because a monomer does not cross-link the ligand, it can be a useful reagent for labeling a mobile ligand without aggregation. To this end, we demonstrated that monomer and A/D dimer are fully capable of interacting with cell-displayed biotinylated receptors without clustering the targets. By fusing the monomer to a fluorescent protein, one may also design a bifunctional molecule that can be used in a variety of labeling studies without chemical conjugation of fluorescent dyes. A stable monomer is also useful in structure–function studies for investigating the role of stability and subunit interaction in biotin affinity. To this end, we provided evidence that the interactions at the A/D dimer interface alone are insufficient to achieve wt affinity. Because monomer and A/D dimer individually have limited affinity, our study suggests the existence of an unknown structural coupling between the subunits that may be investigated in future studies.

ASSOCIATED CONTENT

Supporting Information

Circular dichroism spectra of QMA and wt tetramer (Figure S1), DLS of M5 and A/D dimer (Figure S2), and A/D dimer pull-down assay (Figure S3). This material is available free of charge via the Internet at http://pubs.acs.org.

AUTHOR INFORMATION

Corresponding Author

*Address: 905 Furnas Hall, University at Buffalo, Buffalo, NY 14260. E-mail: sjpark6@buffalo.edu. Phone: (716) 645-1199. Fax: (716) 645-3822.

ACKNOWLEDGMENTS

We thank Cheng Kuo Hsu for assistance with the characterization of A/D dimer. The work was supported in part by the NSF CAREER grant to SP (#1053608). The Zeiss LSM 710 "In Tune" Confocal Microscope used for imaging was purchased through NSF Major Research Instrumentation grant #DBI 0923133.

ABBREVIATIONS

wt, wild-type streptavidin tetramer; CD, circular dichroism spectroscopy; T_m, denaturation temperature; FP, fluorescence polarization spectroscopy; K_d, biotin binding affinity; DLS, dynamic light scattering; rmsd, root-mean-square deviation; SDS–PAGE, sodium dodecyl sulfate–polyacrylamide gel electrophoresis.

REFERENCES

(1) Wilchek, M., and Bayer, E. A. (1990) Introduction to avidin-biotin technology. *Methods Enzymol. 184*, 5–13.
(2) Sano, T., Vajda, S., and Cantor, C. R. (1998) Genetic engineering of streptavidin, a versatile affinity tag. *J. Chromatogr., B: Biomed. Sci. Appl. 715*, 85–91.
(3) Schetters, H. (1999) Avidin and streptavidin in clinical diagnostics. *Biomol. Eng. 16*, 73–78.
(4) Laitinen, O. H., Nordlund, H. R., Hytonen, V. P., and Kulomaa, M. S. (2007) Brave new (strept)avidins in biotechnology. *Trends Biotechnol. 25*, 269–277.
(5) Helppolainen, S. H., Nurminen, K. P., Maatta, J. A., Halling, K. K., Slotte, J. P., Huhtala, T., Liimatainen, T., Yla-Herttuala, S., Airenne, K. J., Narvanen, A., Janis, J., Vainiotalo, P., Valjakka, J., Kulomaa, M. S., and Nordlund, H. R. (2007) Rhizavidin from *Rhizobium etli*: The first natural dimer in the avidin protein family. *Biochem. J. 405*, 397–405.
(6) Helppolainen, S. H., Maatta, J. A., Halling, K. K., Slotte, J. P., Hytonen, V. P., Janis, J., Vainiotalo, P., Kulomaa, M. S., and Nordlund, H. R. (2008) Bradavidin II from *Bradyrhizobium japonicum*: A new avidin-like biotin-binding protein. *Biochim. Biophys. Acta 1784*, 1002–1010.
(7) Maatta, J. A., Helppolainen, S. H., Hytonen, V. P., Johnson, M. S., Kulomaa, M. S., Airenne, T. T., and Nordlund, H. R. (2009) Structural and functional characteristics of xenavidin, the first frog avidin from *Xenopus tropicalis*. *BMC Struct. Biol. 9*, 63.
(8) Sardo, A., Wohlschlager, T., Lo, C., Zoller, H., Ward, T. R., and Creus, M. (2011) Burkavidin: A novel secreted biotin-binding protein from the human pathogen *Burkholderia pseudomallei*. *Protein Expression Purif. 77*, 131–139.
(9) Lindqvist, Y., and Schneider, G. (1996) Protein-biotin interactions. *Curr. Opin. Struct. Biol. 6*, 798–803.
(10) Sano, T., and Cantor, C. R. (1995) Intersubunit contacts made by tryptophan 120 with biotin are essential for both strong biotin binding and biotin-induced tighter subunit association of streptavidin. *Proc. Natl. Acad. Sci. U.S.A. 92*, 3180–3184.
(11) Chilkoti, A., Tan, P. H., and Stayton, P. S. (1995) Site-directed mutagenesis studies of the high-affinity streptavidin-biotin complex: Contributions of tryptophan residues 79, 108, and 120. *Proc. Natl. Acad. Sci. U.S.A. 92*, 1754–1758.
(12) Sano, T., Vajda, S., Smith, C. L., and Cantor, C. R. (1997) Engineering subunit association of multisubunit proteins: A dimeric streptavidin. *Proc. Natl. Acad. Sci. U.S.A. 94*, 6153–6158.
(13) Laitinen, O. H., Airenne, K. J., Marttila, A. T., Kulik, T., Porkka, E., Bayer, E. A., Wilchek, M., and Kulomaa, M. S. (1999) Mutation of a

critical tryptophan to lysine in avidin or streptavidin may explain why sea urchin fibropellin adopts an avidin-like domain. *FEBS Lett. 461*, 52−58.
(14) Pazy, Y., Eisenberg-Domovich, Y., Laitinen, O. H., Kulomaa, M. S., Bayer, E. A., Wilchek, M., and Livnah, O. (2003) Dimer-tetramer transition between solution and crystalline states of streptavidin and avidin mutants. *J. Bacteriol. 185*, 4050−4056.
(15) Meir, A., Helppolainen, S. H., Podoly, E., Nordlund, H. R., Hytonen, V. P., Maatta, J. A., Wilchek, M., Bayer, E. A., Kulomaa, M. S., and Livnah, O. (2009) Crystal structure of rhizavidin: Insights into the enigmatic high-affinity interaction of an innate biotin-binding protein dimer. *J. Mol. Biol. 386*, 379−390.
(16) Laitinen, O. H., Nordlund, H. R., Hytonen, V. P., Uotila, S. T., Marttila, A. T., Savolainen, J., Airenne, K. J., Livnah, O., Bayer, E. A., Wilchek, M., and Kulomaa, M. S. (2003) Rational design of an active avidin monomer. *J. Biol. Chem. 278*, 4010−4014.
(17) Wu, S. C., Ng, K. K., and Wong, S. L. (2009) Engineering monomeric streptavidin and its ligands with infinite affinity in binding but reversibility in interaction. *Proteins 77*, 404−412.
(18) Alberts, B., Johnson, A., Lewis, J., Raff, M., Roberts, K., and Walter, P. (2002) *Molecular Biology of the Cell*, 4th ed., Garland Science, New York.
(19) Howarth, M., Chinnapen, D. J., Gerrow, K., Dorrestein, P. C., Grandy, M. R., Kelleher, N. L., El-Husseini, A., and Ting, A. Y. (2006) A monovalent streptavidin with a single femtomolar biotin binding site. *Nat. Methods 3*, 267−273.
(20) Argarana, C. E., Kuntz, I. D., Birken, S., Axel, R., and Cantor, C. R. (1986) Molecular cloning and nucleotide sequence of the streptavidin gene. *Nucleic Acids Res. 14*, 1871−1882.
(21) Hsu, C. K., and Park, S. (2010) Computational and mutagenesis studies of the streptavidin native dimer interface. *J. Mol. Graphics Modell. 29*, 295−308.
(22) Kale, L., Skeel, R., Bhandarkar, M., Brunner, R., Gursoy, A., Krawetz, N., Phillips, J., Shinozaki, A., Varadarajan, K., and Schulten, K. (1999) NAMD2: Greater scalability for parallel molecular dynamics. *J. Comput. Phys. 151*, 283−312.
(23) MacKerell, A. D., Bashford, D., Bellott, M., Dunbrack, R. L., Evanseck, J. D., Field, M. J., Fischer, S., Gao, J., Guo, H., Ha, S., Joseph-McCarthy, D., Kuchnir, L., Kuczera, K., Lau, F. T. K., Mattos, C., Michnick, S., Ngo, T., Nguyen, D. T., Prodhom, B., Reiher, W. E., Roux, B., Schlenkrich, M., Smith, J. C., Stote, R., Straub, J., Watanabe, M., Wiorkiewicz-Kuczera, J., Yin, D., and Karplus, M. (1998) All-atom empirical potential for molecular modeling and dynamics studies of proteins. *J. Phys. Chem. B 102*, 3586−3616.
(24) Humphrey, W., Dalke, A., and Schulten, K. (1996) VMD: Visual molecular dynamics. *J. Mol. Graphics 14*, 33−38.
(25) Howarth, M., Takao, K., Hayashi, Y., and Ting, A. Y. (2005) Targeting quantum dots to surface proteins in living cells with biotin ligase. *Proc. Natl. Acad. Sci. U.S.A. 102*, 7583−7588.
(26) Wu, S. C., and Wong, S. L. (2005) Engineering soluble monomeric streptavidin with reversible biotin binding capability. *J. Biol. Chem. 280*, 23225−23231.
(27) Chu, V., Freitag, S., Le Trong, I., Stenkamp, R. E., and Stayton, P. S. (1998) Thermodynamic and structural consequences of flexible loop deletion by circular permutation in the streptavidin-biotin system. *Protein Sci. 7*, 848−859.
(28) Freitag, S., Le Trong, I., Klumb, L., Stayton, P. S., and Stenkamp, R. E. (1997) Structural studies of the streptavidin binding loop. *Protein Sci. 6*, 1157−1166.
(29) Minor, D. L. Jr., and Kim, P. S. (1994) Measurement of the β-sheet-forming propensities of amino acids. *Nature 367*, 660−663.
(30) Bai, Y., and Englander, S. W. (1994) Hydrogen bond strength and β-sheet propensities: The role of a side chain blocking effect. *Proteins 18*, 262−266.
(31) Park, S., Boder, E. T., and Saven, J. G. (2005) Modulating the DNA affinity of Elk-1 with computationally selected mutations. *J. Mol. Biol. 348*, 75−83.
(32) Teilum, K., Olsen, J. G., and Kragelund, B. B. (2011) Protein stability, flexibility and function. *Biochim. Biophys. Acta 1814*, 969−976.
(33) Luque, I., and Freire, E. (2000) Structural stability of binding sites: Consequences for binding affinity and allosteric effects. *Proteins Suppl. 4*, 63−71.
(34) Erlanson, D. A., Braisted, A. C., Raphael, D. R., Randal, M., Stroud, R. M., Gordon, E. M., and Wells, J. A. (2000) Site-directed ligand discovery. *Proc. Natl. Acad. Sci. U.S.A. 97*, 9367−9372.
(35) Verdine, G. L., and Norman, D. P. (2003) Covalent trapping of protein-DNA complexes. *Annu. Rev. Biochem. 72*, 337−366.
(36) Buck, E., and Wells, J. A. (2005) Disulfide trapping to localize small-molecule agonists and antagonists for a G protein-coupled receptor. *Proc. Natl. Acad. Sci. U.S.A. 102*, 2719−2724.
(37) Lim, K. H., Madabhushi, S. R., Mann, J., Neelamegham, S., and Park, S. (2010) Disulfide trapping of protein complexes on the yeast surface. *Biotechnol. Bioeng. 106*, 27−41.
(38) Borchert, T. V., Abagyan, R., Jaenicke, R., and Wierenga, R. K. (1994) Design, creation, and characterization of a stable, monomeric triosephosphate isomerase. *Proc. Natl. Acad. Sci. U.S.A. 91*, 1515−1518.
(39) Abdalla, A. M., Bruns, C. M., Tainer, J. A., Mannervik, B., and Stenberg, G. (2002) Design of a monomeric human glutathione transferase GSTP1, a structurally stable but catalytically inactive protein. *Protein Eng. 15*, 827−834.
(40) Aslan, F. M., Yu, Y., Mohr, S. C., and Cantor, C. R. (2005) Engineered single-chain dimeric streptavidins with an unexpected strong preference for biotin-4-fluorescein. *Proc. Natl. Acad. Sci. U.S.A. 102*, 8507−8512.
(41) Pal, D., and Chakrabarti, P. (2000) β-Sheet propensity and its correlation with parameters based on conformation. *Acta Crystallogr. D56*, 589−594.
(42) Kim, C. A., and Berg, J. M. (1993) Thermodynamic β-sheet propensities measured using a zinc-finger host peptide. *Nature 362*, 267−270.
(43) Smith, C. K., Withka, J. M., and Regan, L. (1994) A thermodynamic scale for the β-sheet forming tendencies of the amino acids. *Biochemistry 33*, 5510−5517.
(44) Makhatadze, G. I., Loladze, V. V., Ermolenko, D. N., Chen, X., and Thomas, S. T. (2003) Contribution of surface salt bridges to protein stability: Guidelines for protein engineering. *J. Mol. Biol. 327*, 1135−1148.
(45) Kumar, S., and Nussinov, R. (1999) Salt bridge stability in monomeric proteins. *J. Mol. Biol. 293*, 1241−1255.
(46) Campion, S. R., Geck, M. K., and Niyogi, S. K. (1993) Cumulative effect of double-site mutations of human epidermal growth factor on receptor binding. *J. Biol. Chem. 268*, 1742−1748.
(47) Marra, E., Azzariti, A., Giannattasio, S., Doonan, S., and Quagliariello, E. (1995) Cumulative effects of mutations in newly synthesised mitochondrial aspartate aminotransferase on uptake into mitochondria. *Biochem. Biophys. Res. Commun. 214*, 511−517.
(48) Pokkuluri, P. R., Raffen, R., Dieckman, L., Boogaard, C., Stevens, F. J., and Schiffer, M. (2002) Increasing protein stability by polar surface residues: Domain-wide consequences of interactions within a loop. *Biophys. J. 82*, 391−398.
(49) Katz, B. A. (1997) Binding of biotin to streptavidin stabilizes intersubunit salt bridges between Asp61 and His87 at low pH. *J. Mol. Biol. 274*, 776−800.
(50) Green, N. M. (1975) Avidin. *Adv. Protein Chem. 29*, 85−133.
(51) Gonzalez, M., Argarana, C. E., and Fidelio, G. D. (1999) Extremely high thermal stability of streptavidin and avidin upon biotin binding. *Biomol. Eng. 16*, 67−72.
(52) Gonzalez, M., Bagatolli, L. A., Echabe, I., Arrondo, J. L., Argarana, C. E., Cantor, C. R., and Fidelio, G. D. (1997) Interaction of biotin with streptavidin. Thermostability and conformational changes upon binding. *J. Biol. Chem. 272*, 11288−11294.